Refinement was carried out by full-matrix least-squares techniques, with all non-hydrogen atoms being assigned anisotropic temperature factors. The positions of some hydrogen atoms were determined from difference Fourier maps; those for others were generated by standard geometric considerations. All hydrogen atoms were assigned an isotropic temperature factor of 5.0 Å^2. The positional parameters of those attached to the rings were included in the least squares. An empirical adsorption correction[41] was applied to the data. Weights used were of the type $w = 1/[\sigma^2(F_o + 0.04F^2)]$. Refinement converged at an unweighted R of 0.057 and an R_w of 0.073, where $R_w = [\sum w(|F_o| - |F_c|)^2/\sum|F_o|^2]^{1/2}$. The maximum shift/error was 0.02. The final difference Fourier showed maximum and minimum electron densities of +0.4e and −0.36e, respectively. Tables of anisotropic thermal parameters, hydrogen atom positions, and structure factors have been deposited as supplementary material.

Molecular Modeling. Interactive computer graphics techniques were used to dock the structure of compound **1** into a model of duplex DNA with an intercalation site. This model is of the alternating hexanucleotide sequence d(TACGTA) and has an intercalation site between the central CG base pairs. It has been constructed by means of least-squares fitting of B-DNA residues to both ends of the CG dinucleoside geometry found in its crystalline complex with proflavine, followed by energy minimization. The docking of compound **1** was performed on a Silicon Graphics IRIS work station with the GEMINI molecular graphics program.[42] The docking process was accompanied by alterations in the conformation of the ligand's side chains. Positions of potential low energy, as judged by maximum stacking of the rings of **1** with base pairs together with minimal repulsive close contacts, were located and subjected to molecular mechanics conjugate gradients full-geometry minimization. The force field used is of the form $E(\text{total}) = E(\text{nonbonded}) + E(\text{electrostatic}) + E(\text{torsion}) + E(\text{angle}) + E(\text{bond})$. The parameter set used for the DNA was the all-atom representation published by Kollman et al.[43] Partial charges for the cation of **1** were obtained by CNDO/2 calculations. Geometry was taken directly from the X-ray analysis reported here. Force constants and torsional potentials for the bond and atom types of **1** not represented in the published tables,[43] especially for aliphatic C–S and N–C, were assigned according to established procedures.[43,44] A distance-dependent dielectric constant was used, of the form $\epsilon = 4r_{ij}$. Convergence was judged to have been achieved during the energy refinement when the rms value of the first derivative was less than 0.15.

Acknowledgment. This work was supported by NSF Grant DBM-8603566 (W.D.W.), a NATO Travel Award (W.D.W. and S.N.), American Cancer Society Grant CH383 (L.S.), the Greenwall Foundation, Inc., Research Corp. (L.S.), ACS-PRF Grant 18704 (L.S.), NIH Grant S07-RR07171 (W.D.W. and L.S.), and the Cancer Research Campaign (S.N.). The 400-MHz NMR spectrometer was obtained with partial support from a Departmental NSF Grant. We thank Professor David Boykin and Dr. T. C. Jenkins for helpful discussions and Dr. I. Haneef for supplying us with his molecular mechanics program.

Registry No. **1**, 117269-54-2; **2**, 117308-21-1; **3**, 90944-65-3; **5**, 117269-55-3; **6**, 117269-56-4; d(TACGTA), 100443-41-2; pyrimidine, 289-95-2; 5-methylpyrimidine, 2036-41-1.

Supplementary Material Available: Tables of hydrogen atom positions and anisotropic thermal parameters (3 pages); listing of observed and calculated structure factors (18 pages). Ordering information is given on any current masthead page.

(41) Walker, N.; Stuart, D. *Acta Crystallogr.* **1983**, *A34*, 1518–166.
(42) *The GEMINI Molecular Graphics Package*; Institute of Cancer Research: Sutton, U.K., 1988.
(43) Weiner, S. J.; Kollman, P. A.; Nguyen, D. T.; Case, D. A. *J. Comput. Chem.* **1986**, *7*, 230–252.
(44) Abraham, Z. H. L.; Agbandje, M.; Neidle, S., to be submitted for publication.

Time-Resolved Observation of Excitation Hopping between Two Identical Chromophores Attached to Both Ends of Alkanes

Tomiki Ikeda,*,† Bong Lee,† Seiji Kurihara,† Shigeo Tazuke,*,† Shinzaburo Ito,‡ and Masahide Yamamoto‡

Contribution from the Photochemical Process Division, Research Laboratory of Resources Utilization, Tokyo Institute of Technology, 4259 Nagatsuta, Midori-ku, Yokohama 227, and Department of Polymer Chemistry, Kyoto University, Kyoto 606, Japan.
Received October 13, 1987

Abstract: Excitation hopping between two identical chromophores has been directly observed by time-resolved fluorescence anisotropy ($r(t)$) measurements with the aid of a picosecond time-correlated single-photon counting system (fwhm 80 ps). In order to explore the excitation hopping behavior *in purely isolated two identical chromophoric systems*, we used α,ω-bis(2-naphthyl)-*n*-alkanes, Nap$(CH_2)_n$Nap (N*n*), where n = 3, 5, 7, and 12, as well as 2-ethylnaphthalene (EN) as a model compound. We show that $r(t)$ for EN does not change with time while $r(t)$ for N*n* decays with time, depending on n, and the initial decay of $r(t)$ becomes faster with decreasing n. Our results clearly indicate that excitation hopping takes place between the two naphthyl moieties attached to both ends of the alkyl chain. Theoretical treatment assuming forward and backward excitation hopping between the two naphthyl moieties has been carried out on the basis of the conformational analysis of N*n*'s, which manifested the distribution function of interchromophore distance and mutual orientation of the two naphthyl moieties. Results of the theoretical treatment have shown to account fairly well for the experimentally observed anisotropy decays.

Electronic excitation transport in molecular aggregate systems has become an area of challenge from both theoretical[1-3] and experimental[4-10] points of view. Since the excitation transport is essentially a phenomenon occurring in a pair of chromophores, the simplest case for the excitation transport in the molecular aggregate systems may be a bichromophoric system. Excitation transport between two nonidentical chromophores was easily

† Tokyo Institute of Technology.
‡ Kyoto University.

(1) (a) Pearlstein, R. M. *J. Chem. Phys.* **1972**, *56*, 2431. (b) Hemenger, R. P.; Pearlstein, R. M. *Ibid.* **1973**, *59*, 4064. (c) Haan, S. W.; Zwanzig, R. *Ibid.* **1978**, *68*, 1879. (d) Blumen, A.; Manz, J. *Ibid.* **1979**, *71*, 4694. (e) Godzik, K.; Jortner, J. *Ibid.* **1980**, *72*, 4471. (f) Blumen, A.; Klafter, J.; Silbey, R. *Ibid.* **1980**, *72*, 5320.

0002-7863/88/1510-8299$01.50/0

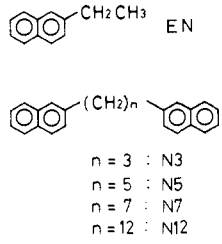

Figure 1. Structures of bichromophoric compounds used in this study.

explored through observation of the sensitized fluorescence of the acceptor,[11] while excitation transport between two identical chromophores cannot be observed by such a conventional method.

The fluorescence depolarization method has been proved to provide unequivocal evidence for excitation transport in the molecular aggregate systems, and many theoretical treatments relating the excitation transport behavior to fluorescence anisotropy have been reported.[2] In fact, validity of this method has been demonstrated in concentrated dye solutions,[7,8] micelles solubilizing dye molecules,[9] and polymers.[10] Furthermore, Moog et al. investigated by time-resolved fluorescence depolarization method excitation transport behavior in a synthetic chlorophyllide-substituted hemoglobin where two pyrochlorophyllides (donor) and two deoxy hemes (acceptor) were located in close proximity.[12]

We report here the direct observation of excitation hopping between two identical chromophores by the time-resolved fluorescence anisotropy [$r(t)$] measurements with the aid of a picosecond time-correlated single-photon counting system. In order to explore the excitation hopping behavior *in purely isolated two identical chromophoric systems*, we used α,ω-bis(2-naphthyl)-*n*-alkanes, Nap$(CH_2)_n$Nap (N*n*), where n = 3, 5, 7, and 12, as well as 2-ethylnaphthalene (EN) as a model compound. Our results clearly indicate that excitation hopping takes place between the two naphthyl moieties attached to both ends of the alkyl chain.

Because of the flexible nature of the links between the two naphthyl moieties, distribution was naturally expected for interchromophore distance and orientation of the two chromophores. In order to analyze the time-resolved measurements on excitation hopping quantitatively, the distribution of the interchromophore distance and the orientation of the two chromophores was evaluated by conformational analysis of the bichromophoric compounds. Calculation of potential energy of nonbonded atoms (van der Waals potential) enabled us to estimate the distribution functions of the interchromophore distance in N3, N5, and N7 and of the orientation of the two naphthyl groups in those molecules. The experimental results of the time-resolved measurements on $r(t)$ of N*n*'s were analyzed on the basis of Förster's mechanism on energy transfer as well as the conformational analyses of those molecules. Theoretical treatment, assuming forward and backward excitation hopping between the two naphthyl moieties, was found to account fairly well for the experimentally observed anisotropy decays.

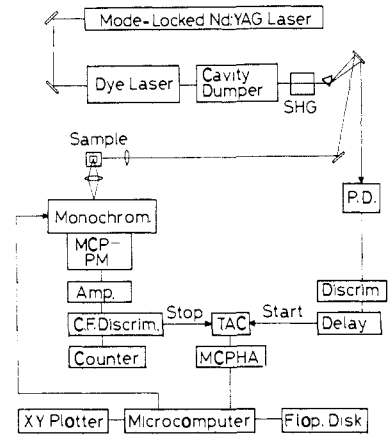

Figure 2. Schematic diagram for picosecond time-resolved fluorescence measurements: PD, photodiode; MCP-PM, microchannel-plate photomultiplier; MCPHA, multichannel pulse-height analyzer.

Experimental Section

2-Ethylnaphthalene (EN) was obtained from Tokyo Kasei and used after purification by distillation under reduced pressure. 1,3-Bis(2-naphthyl)propane (N3) was prepared and purified as reported previously.[13] Structure of the bichromophoric compounds used in this study is shown in Figure 1.

1,5-Bis(2-naphthyl)pentane (N5). A mixture of 2-naphthaldehyde (0.1 mol) and acetone (0.05 mol) in ethanol (200 mL) was added to a solution of sodium hydroxide (30 g) in ethanol, and the resulting mixture was left with stirring for 1 h. An insoluble yellow product formed was filtered, washed with water, and recrystallized from benzene/chloroform, giving yellow crystalline 1,5-bis(2-naphthyl)-1,4-pentadien-3-one, mp 241–243 °C.

This compound was reduced with zinc dust in acetic acid by the same procedure as for N3. The extracted product was crystallized from ethanol, giving colorless crystalline 1,5-bis(2-naphthyl)-3-pentanone: mp 126–127 °C; IR (KBr) 3050, 2950, 1685, 1600, 825, 735, 470 cm^{-1}. Anal. Calcd for $C_{25}H_{22}O$: C, 88.72; H, 6.55; O, 4.72. Found: C, 88.98; H, 6.50; O, 4.93.

This ketone was reduced with hydrazine and sodium hydroxide in triethylene glycol. The reaction mixture was extracted with benzene, and the residue was purified by chromatography on silica gel with benzene/hexane (1/9) as eluent. The colorless crystal of N5 was obtained by recrystallization from ethanol: mp 92–93 °C; IR (KBr) 3050, 2950, 2850, 1600, 820, 740, 480 cm^{-1}. ^1H NMR (CS_2) δ 1.3–1.9 (m, 3), 2.71 (t, 2, J = 7 Hz), 7.1–7.7 (m, 7). Anal. Calcd for $C_{25}H_{24}$: C, 92.54; H, 7.46. Found: C, 92.53; H, 7.59.

1,7-Bis(2-naphthyl)heptane (N7). N7 was synthesized by Grignard reaction between 2-naphthonitrile and dibromopentane, followed by reduction. A solution of 1,5-dibromopentane (8 g) in dry ether was added dropwise to a stirred dispersion of magnesium (2.5 g) in dry ether (25 mL). After the mixture refluxed for 1 h, a solution of 2-naphthonitrile (10 g) in dry tetrahydrofuran (THF; 50 mL) was added dropwise. The resulting mixture was then refluxed for 4 h after removal of ether from the reaction mixture. After the mixture was cooled in an ice bath, 6 N hydrochloric acid (80 mL) was added, and the solution was refluxed for 7 h after removal of THF from the solution. The reaction mixture was extracted with dichloromethane and washed with water. The crude product was purified by column chromatography on silica gel with dichloromethane as eluent and then recrystallized from ethanol. The colorless crystalline 1,5-bis(2-naphthoyl)pentane was obtained: mp 119–120 °C; IR (KBr) 3050, 2950, 1680, 1625, 810, 740, 490 cm^{-1}.

The ketone was reduced by the same method as N5, and the product was purified by column chromatography on silica gel and then recrystallized from methanol. The colorless crystalline N7 was obtained: mp 78–79 °C; IR (KBr) 3050, 2930, 2850, 1600, 820, 740, 480 cm^{-1}; ^1H

(2) (a) Gochanour, C. G.; Andersen, H. C.; Fayer, M. D. *J. Chem. Phys.* **1979**, *70*, 4254. (b) Loring, R. F.; Andersen, H. C.; Fayer, M. D. *Ibid.* **1982**, *76*, 2015. (c) Ediger, M. D.; Fayer, M. D. *Ibid.* **1983**, *78*, 2518. (d) Peterson, K. A.; Fayer, M. D. *Ibid.* **1986**, *85*, 4702. (e) Baumann, J.; Fayer, M. D. *Ibid.* **1986**, *85*, 4087.

(3) (a) Fredrickson, G. H.; Andersen, H. C.; Frank, C. W. *Macromolecules* **1983**, *16*, 1456. (b) Fredrickson, G. H.; Andersen, H. C.; Frank, C. W. *Ibid.* **1984**, *17*, 54. (c) Fredrickson, G. H.; Andersen, H. C.; Frank, C. W. *Ibid.* **1984**, *17*, 1496.

(4) (a) Blanzat, B.; Barthou, C.; Tercier, N.; Andre, J.-J.; Simon, J. *J. Am. Chem. Soc.* **1987**, *109*, 6193. (b) Markovitsi, D.; Tran-Thi, T.-H.; Briois, V.; Simon, J.; Ohta, K. *Ibid.* **1988**, *110*, 2001. (c) Tamai, N.; Yamazaki, T.; Yamazaki, I. *J. Phys. Chem.* **1987**, *91*, 841. (d) Baeyens-Volant, D.; David, C. *Mol. Cryst. Liq. Cryst.* **1985**, *116*, 217.

(5) Soutar, I.; Phillips, D. In *Photophysical and Photochemical Tools in Polymer Science*; Winnik, M. A., Ed.; Reidel: Dordrecht, The Netherlands, 1986; p 97.

(6) Morrison, H.; Pandey, G. *Chem. Phys. Lett.* **1983**, *96*, 126.

(7) Gochanour, C. R.; Fayer, M. D. *J. Phys. Chem.* **1981**, *85*, 1989.

(8) Hart, D. E.; Anfinrud, P. A.; Struve, W. S. *J. Chem. Phys.* **1987**, *86*, 2689.

(9) Ediger, M. D.; Domingue, R. P.; Fayer, M. D. *J. Chem. Phys.* **1984**, *80*, 1246.

(10) (a) Ediger, M. D.; Fayer, M. D. *Macromolecules* **1983**, *16*, 1839. (b) Ediger, M. D.; Domingue, R. P.; Peterson, K. A.; Fayer, M. D. *Ibid.* **1985**, *18*, 1182. (c) Peterson, K. A.; Zimmt, M. B.; Linse, S.; Domingue, R. P.; Fayer, M. D. *Ibid.* **1987**, *20*, 168.

(11) Stryer, L.; Haughland, R. *Proc. Natl. Acad. Sci.* **1967**, *58*, 719.

(12) Moog, R. S.; Kuki, A.; Fayer, M. D.; Boxer, S. G. *Biochemistry* **1984**, *23*, 1564.

(13) Chandross, E. A.; Dempster, C. J. *J. Am. Chem. Soc.* **1970**, *2*, 2374.

NMR (CS_2) δ 1.2–1.5 (m, 3), 1.5–1.8 (m, 2), 2.70 (t, 2, J = 7 Hz), 7.1–7.7 (m, 7). Anal. Calcd for $C_{27}H_{28}$: C, 91.99; H, 8.00. Found: C, 91.86; H, 8.00.

1,12-Bis(2-naphthyl)dodecane (N12). N12 was prepared by the same method as that for N7. 1,10-Dibromodecane was used instead of 1,5-dibromopentane. The crude product was recrystallized from ethanol, giving the colorless crystalline N12: mp 93–94 °C; IR (KBr) 3050, 2910, 2850, 1600, 820, 740, 480 cm^{-1}; ^1H NMR (CS_2) δ 1.15–1.48 (m, 8), 1.48–1.84 (m, 2), 2.70 (t, 2, J = 7 Hz), 7.1–7.7 (m, 7). Anal. Calcd for $C_{32}H_{38}$: C, 90.94; H, 9.06. Found: C, 90.48; H, 9.15.

2-Methyltetrahydrofuran (MTHF) was used in the spectroscopic measurements throughout this work. MTHF (Tokyo Kasei) was washed with 10% NaOH, dried over $MgSO_4$ and then CaH_2, and finally distilled fractionally over sodium metal twice.

Measurements. A time-correlated, single-photon counting method was used to measure the fluorescence and the fluorescence anisotropy decays (Figure 2). A synchronously pumped, cavity-dumped dye laser (Spectra Physics 375B and 344S) operated with a mode-locked Nd:YAG laser (Spectra Physics 3460 and 3240) was an excitation pulse source with a pulse width of 6 ps (fwhm). For excitation of samples, frequency doubling was achieved with a KDP crystal (Inrad 531). Fluorescence was monitored at right angles to the excitation path through a monochromator (Jasco CT-25C) by a microchannel-plate photomultiplier (Hamamatsu R1564U-01). Signals from the photomultiplier were amplified with a 1.3 GHz preamplifier (HP 8447D), discriminated with a constant fraction discriminator (Ortec 583), and used as a stop pulse for a time-to-amplitude converter (TAC; Ortec 457). A start pulse was provided from a fast photodiode (Antel AR-S2) monitoring a laser pulse through a discriminator (Ortec 436). Data from the TAC were stored in a multichannel analyzer (Canberra 35 Plus) and then transferred to a microcomputer (NEC PC9801) where decay analysis was performed by an iterative nonlinear least-squares method.[14]

For anisotropy decay measurements, a vertically polarized excitation light pulse was obtained through a Babinet–Soleil compensator, and $I_\parallel(t)$ and $I_\perp(t)$ were measured alternatively through a polarizer, which was placed in front of the monochromator. Here, $I_\parallel(t)$ and $I_\perp(t)$ represent the fluorescence intensities observed with parallel and perpendicular orientation of the polarizer to the excitation pulse. $I_\parallel(t)$ and $I_\perp(t)$ were measured alternatively by rotating the polarizer periodically in order to eliminate any artifacts due to long-term laser instability. A depolarizer was also placed just before the monochromator to remove anisotropic characteristics of the monochromator against $I_\parallel(t)$ and $I_\perp(t)$. The fluorescence anisotropy, $r(t)$, was calculated by eq 1 where deconvolution

$$r(t) = [I_\parallel(t) - I_\perp(t)]/[I_\parallel(t) + 2I_\perp(t)] \quad (1)$$

of the instrument response function was performed.[14] In every run, more than 50 000 counts were accumulated at the maximum channel to ensure reliable values of $r(t)$. Decay of $r(t)$ was analyzed by eq 2 on the basis

$$r(t) = A \exp(-2\omega t) + B \quad (2)$$

of the iterative least-squares method (see the Discussion). In the fluorescence and the fluorescence anisotropy decay analyses, goodness of the fitting was judged by reduced χ^2 and Durbin–Watson (DW) parameters.[14]

Corrected fluorescence and excitation spectra were taken under argon atmosphere on a Hitachi F-4000 fluorescence spectrometer. In order to exclude the contribution of rotational diffusion of the chromophores to the fluorescence depolarization, both the steady-state and time-resolved fluorescence anisotropy measurements were performed at 77 K in glass matrix of MTHF at the concentration of 10^{-5} M.

Conformational Analysis. Conformational analysis was performed on the basis of potential energy calculation including the van der Waals interaction between nonbonded atoms and the intrinsic torsional potential energies associated with rotation about C–C bonds.[15-18] For calculation of the van der Waals interaction, the Lennard–Jones potential function was employed in which the potential energy V_{ij} between the ith and jth nonbonded atoms is expressed by eq 3 where d_{ij} is the distance between

$$V_{ij} = B_{ij}/d_{ij}^{12} - A_{ij}/d_{ij}^{6} \quad (3)$$

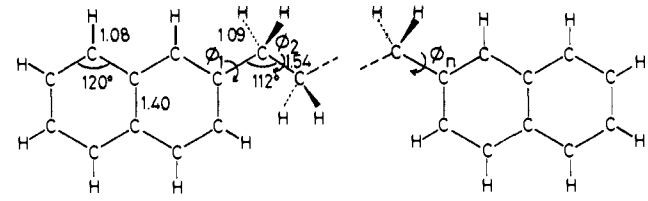

Figure 3. Structural parameters of Nn used for the conformational analysis.

Table I. Analysis of Fluorescence Decay Profiles of Nn and EN[a]

	A	τ	χ^2	DW
EN	0.363	80.5	1.0345	1.8785
N3	0.365	81.0	1.0890	1.7202
N5	0.296	80.0	0.9239	1.8628
N7	0.409	79.6	1.0137	1.9965
N12	0.385	81.3	0.9751	1.7937

[a] λ_{ex} = 318 nm, λ_{em} = 335 nm; measured in MTHF at 77 K; analysis based on $I(t) = A \exp(-t/\tau)$.

the ith and jth nonbonded atoms and A_{ij} and B_{ij} are coefficients.[16] The attractive term coefficient A_{ij} in eq 3 can be determined by applying the Slater–Kirkwood equation modified by Scott and Scheraga,[19] but in this study we adopted the A_{ij} and B_{ij} values reported in the literature.[16] The potential function was modified by considering the molecule–solvent interaction according to the procedure employed by Flory.[20] For molecules in a solvent, intramolecular contact with an alteration in the molecular conformation occurs at the expense of intermolecular interaction with the solvent. The molecule–solvent interaction is attractive, so that inclusion of this effect would result in suppression of the attractive term in eq 3 at larger distances, leading to effective elimination of the minimum in the function. This means that calculations can be performed by the potential functions given in eq 4 where V_{ij}^0 is the value of V_{ij} at

$$V_{ij}^* = V_{ij} - V_{ij}^0 \qquad d_{ij} < d_{ij}^0$$
$$V_{ij}^* = 0 \qquad d_{ij} \geq d_{ij}^0 \quad (4)$$

$d_{ij} = d_{ij}^0$ (the sum of the van der Waals radii of the interacting atoms). The total potential energy due to the van der Waals interaction was calculated as the sum over all pairs of nonbonded atoms. The intrinsic torsional potential energy for the skeletal alkyl chain, $E_{tor}(\phi)$, was calculated for the rotational angle ϕ by eq 5 where E_0 is the torsional barrier

$$E_{tor}(\phi) = (E_0/2)(1 + \cos 3\phi) \quad (5)$$

energy (E_0 = 2.8 kcal/mol).[21] The torsional energy for the rotation of the naphthalene ring was neglected.[17a] The total potential energy was obtained as the sum of the potential energies due to the van der Waals interaction and the intrinsic torsional potentials.

Structural parameters used in this calculation are shown in Figure 3. The parameters for the naphthyl moiety were obtained from X-ray data of naphthalene crystal,[22] and those of skeletal alkane chain were those used by Abe et al.[21] For the calculation of the potential energies of the Nn compound, n + 1 rotational angles, ϕ_1, ϕ_2, ..., ϕ_{n+1}, were taken into account (Figure 3).

Results

Fluorescence Spectra and Fluorescence Lifetimes. All samples used in this study (EN and Nn's) showed nearly identical absorption spectra (λ_{max} = 276 nm (^1L_a) and 319 nm (^1L_b)) and emission spectra (λ_{max} = 322 nm) in MTHF except N3, which exhibited excimer fluorescence with a peak at 400 nm at room temperature. However, in a rigid matrix at 77 K all the samples showed nearly identical fluorescence (λ_{max} = 319 nm) and excitation spectra (λ_{max} = 318 nm (^1L_b)), indicating that the ground-state interaction is negligible in all compounds.

In Figure 4 are shown a fluorescence decay profile of N5 measured at 77 K in the glass matrix and the instrument response function (80-ps fwhm) as an example of the fluorescence decay analysis. The fluorescence decay of N5 could be analyzed by a single exponential function with a lifetime (τ) of 80.0 ns. Results

(14) O'Connor, D. V.; Phillips, D. *Time-Correlated Single Photon Counting*; Academic: New York, 1984.
(15) Flory, P. J. *Statistical Mechanics of Chain Molecules*; Wiley: New York, 1969.
(16) Hopfinger, A. J. *Conformational Properties of Macromolecules*; Academic: New York, 1973.
(17) (a) Ito, S.; Yamamoto, M.; Nishijima, Y. *Bull. Chem. Soc. Jpn.* **1982**, *55*, 363. (b) Kanaya, T.; Hatano, Y.; Yamamoto, M.; Nishijima, Y. *Ibid.* **1979**, *52*, 2079.
(18) Takenaka, A.; Sasada, Y. *J. Cryst. Soc. Jpn.* **1980**, *22*, 214.
(19) Scott, R. A.; Scheraga, H. A. *J. Chem. Phys.* **1965**, *42*, 2209.
(20) Brant, D. A.; Flory, P. J. *J. Am. Chem. Soc.* **1965**, *87*, 2791.
(21) Abe, A.; Jernigan, R. L.; Flory, P. J. *J. Am. Chem. Soc.* **1966**, *88*, 631.
(22) Brock, C. P.; Dunitz, J. D. *Acta Crystallogr.* **1982**, *B38*, 2218.

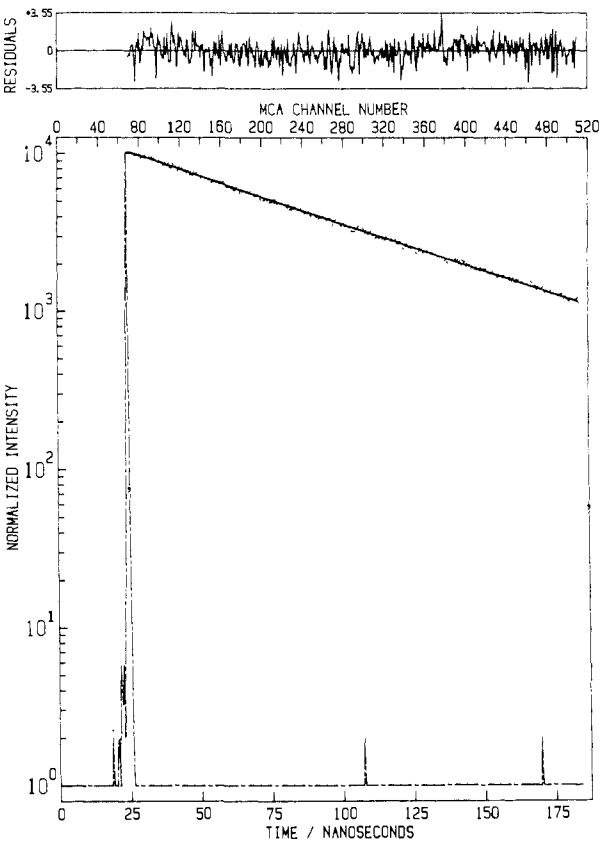

Figure 4. Fluorescence decay profile of N5 in MTHF at 77 K: λ_{ex} = 318 nm, λ_{em} = 335 nm.

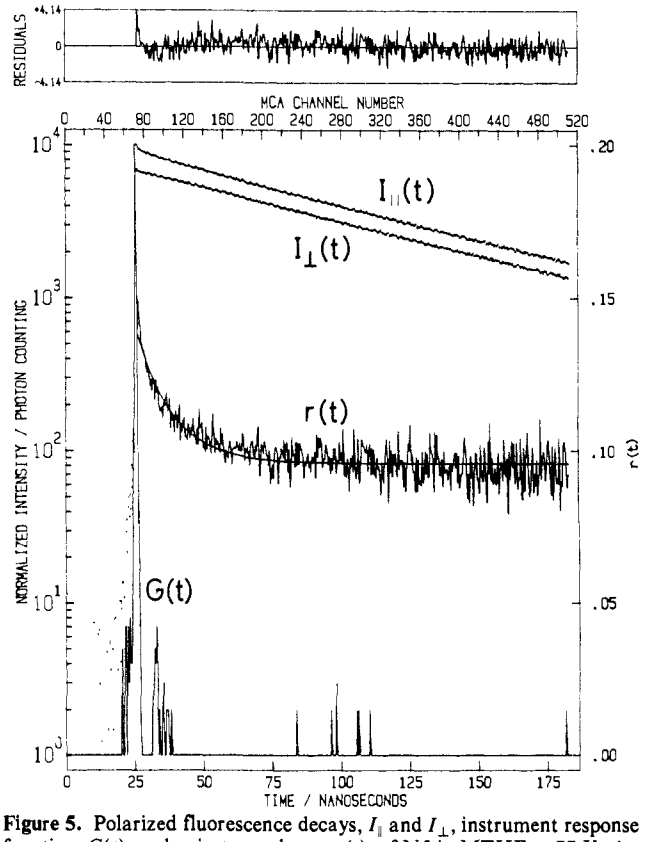

Figure 5. Polarized fluorescence decays, $I_{\parallel}$ and $I_{\perp}$, instrument response function, $G(t)$, and anisotropy decay, $r(t)$, of N5 in MTHF at 77 K: λ_{ex} = 318 nm, λ_{em} = 335 nm.

of the decay analyses of Nn's are summarized in Table I, which indicates that, in all compounds, the decays were analyzed satisfactorily by a single exponential function with $\tau \sim 80$ ns as judged by reduced χ^2 and Durbin–Watson (DW) parameters.[14]

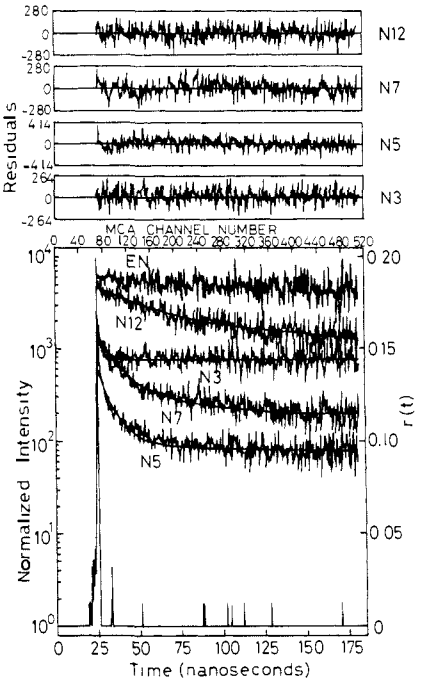

Figure 6. Anisotropy decays of Nn's and EN and the best fit curves based on $r(t) = A \exp(-2\omega t) + B$. Measured in MTHF at 77 K: λ_{ex} = 318 nm, λ_{em} = 335 nm.

Table II. Excitation Hopping Parameters Obtained by the Best Fit Curves[a]

	A	B	ω, s^{-1}	χ^2	DW
N3	0.16	0.14	1.8×10^8	0.8586	1.8512
N5	0.14	0.10	4.1×10^7	1.0487	1.7363
N7	0.15	0.12	1.9×10^7	0.8421	1.8153
N12	0.18	0.15	6.8×10^6	0.8119	1.9407

[a] Fitting of the experimentally observed decay curves (Figure 6) with eq 2, $r(t) = A \exp(-2\omega t) + B$.

This result shows that the properties of the excited states are quite similar among the bichromophoric compounds and their model compound, EN, and there is no specific interaction leading to the deactivation of the excited states of the naphthyl moieties.

Fluorescence Anisotropy Decays. In Figure 5 are shown $I_{\parallel}(t)$, $I_{\perp}(t)$, and $r(t)$ of N5 measured at 77 K as a function of time, and the anisotropy decays for all compounds are shown in Figure 6. It is clear that $r(t)$ for EN does not change with time, which is an explicit piece of evidence that excitation remains at the initially excited sites during its lifetime. In contrast, in bichromophoric compounds, the decays of $r(t)$ are clearly observed. This means that emission from a transition moment, which is different from that of the originally excited chromophore, contributes to the observed emission. Furthermore, with decreasing alkyl chain length, the initial decay of $r(t)$ becomes faster. These results indicate that excitation hopping takes place between the two naphthyl moieties attached to both ends of the alkyl chain.

In Figure 6 are also shown the best fit curves based on eq 2 and on top the residuals for each fit. Three parameters (A, B, and ω) obtained by the fitting procedure are listed in Table II.

Conformational Analysis. A conformational energy map for N3 is shown in Figure 7 as a function of ϕ_2 and ϕ_3 where ϕ_1 and ϕ_4 were fixed at 90°.[17a] This energy map was prepared from the results of the potential energy calculation at intervals of 5° for ϕ_2 and ϕ_3. Contours are shown at intervals of 0.5 kcal/mol relative to the energy minima indicated by ×. The fraction of the ith conformation, f_i, was calculated by the following equation on the assumption that the distribution of conformations obeys the Boltzmann distribution (eq 6) where E_i is the calculated potential

$$f_i = \exp(-E_i/RT)/\sum_i \exp(-E_i/RT) \qquad (6)$$

energy for the ith conformation.[17b] On every conformation, the

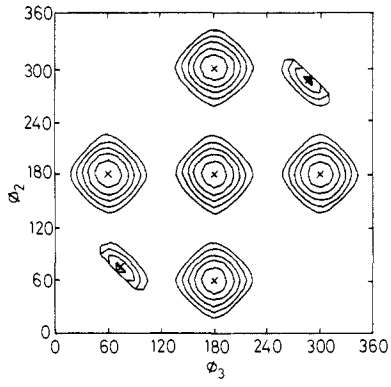

Figure 7. Conformational energy map for N3 as a function of ϕ_2 and ϕ_3. ϕ_1 and ϕ_4 were fixed at 90°. Contours are shown at intervals of 0.5 kcal/mol relative to the energy minima indicated by ×.

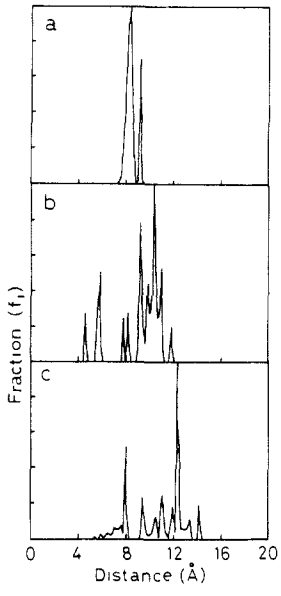

Figure 8. Distribution functions of interchromophore distance for N3 (a), N5 (b), and N7 (c) at 77 K.

interchromophore distance (R) and the angle between two vectors along the long axis of the naphthalene rings (θ_L) and along the short axis of the naphthalene ring (θ_S) were calculated, and the distribution functions for R, θ_L, and θ_S were evaluated on the basis of eq 6. Here, R was defined as the distance between the centers of the two naphthalene rings.

Potential energy calculations on N5 and N7 was carried out in the same way as that for N3, while the interval of calculation for N5 (ϕ_2–ϕ_5) and N7 (ϕ_2–ϕ_7) was 60° and 120°, respectively. The model considered for N7 is the rotational isomeric state model where all C–C bonds of the methylene chain are assumed to be one of three rotational isomers: trans, gauche(+), and gauche(−). Feasibility of this model for rather short polymethylene chains like those considered here has been explored extensively.[23]

Distribution functions of interchromophore distance (R) for N3, N5, and N7 at 77 K are shown in Figure 8 where calculation of the distribution was performed at a 0.2-Å increment. It is clearly seen that in N3 the distribution of R is quite narrow at 77 K and bimodal with two maxima at R = 8.4 Å and at R = 9.2 Å, though at room temperature (i.e. at 300 K) the distribution was much broader (data not shown). A fraction of the stable conformers with R = 8.2 ± 0.4 Å is more than 0.8, and that with R = 9.2 Å, which corresponds to a conformation with the all-trans configuration in the skeleton chain (ϕ_2 = ϕ_3 = 180°), is less than 0.2. In N5 and N7, the distribution is broader as expected from the increased number of the skeletal atoms. In N5, there are several maxima, however, significant fraction lies at R = 5.7 ± 0.1 Å (0.13), at R = 9.2 ± 0.2 Å (0.18), and at R = 10.4 ± 0.6 Å (0.52). In N7, the distribution is broadest, but the maxima lie at R = 8.0 ± 0.1 Å (0.13) and at R = 12.4 ± 0.2 Å (0.27). An ensemble-averaged interchromophore distance, $\langle R \rangle$, was calculated by eq 7 where R_i is the interchromophore distance of

$$\langle R \rangle = \sum_i R_i f_i(R_i) / \sum_i f_i(R_i) \qquad (7)$$

the ith conformer and $f_i(R_i)$ is the fraction of the ith conformers. The $\langle R \rangle$ values calculated were 8.41 Å for N3, 9.15 Å for N5, and 10.79 Å for N7.

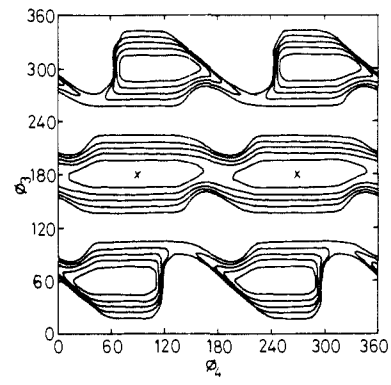

Figure 9. Conformational energy map for N3 as a function of ϕ_3 and ϕ_4. ϕ_1 and ϕ_2 were fixed at 90° and 180°. Contours are shown at intervals of 0.5 kcal/mol relative to the energy minima indicated by ×.

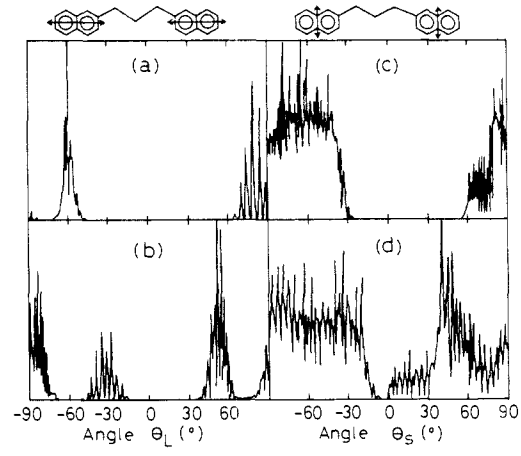

Figure 10. Angular distributions of the two vectors along the long axis (θ_L) and the short axis (θ_S) of the naphthalene rings in N3. (a) and (b) are for θ_L, and (c) and (d) are for θ_S. (a) and (c) were computed with fixed rotational angles of ϕ_1 = ϕ_4 = 90°, and (b) and (d), with ϕ_1 = 90° and ϕ_2 = 180°.

A conformational energy map for N3 calculated as a function of ϕ_3 and ϕ_4 is shown in Figure 9 where ϕ_1 and ϕ_2 were fixed at 90° and 180°, respectively, and calculation was performed at 5° intervals. Figure 9 shows a remarkable feature, that the potential energy of N3 is insensitive to the rotation of the naphthalene ring (ϕ_4), while the potential energy exhibits three clear minima on the rotation of the skeleton bond (ϕ_3), which corresponds to the hree rotational isomers. Furthermore, our calculation has shown that the interchromophore distance of N3 is similarly insensitive to the rotation of the naphthalene ring (data not shown). This may be due to the position of substitution in the naphthalene ring. Angular distribution of θ_L and θ_S at 77 K is shown in Figure 10 where (a) and (b) indicate the distribution of θ_L and (c) and (d) are those of θ_S. These angular distribution functions were computed on the basis of the two different potential energy calculations: one with fixed rotational angles of ϕ_1 = ϕ_4 = 90° (a and c) and the other with ϕ_1 = 90° and ϕ_2 = 180° (b and d). Comparison of Figures 8 and 10 reveals a quite interesting characteristic of α,ω-bis(*2-naphthyl*)propane, that the distribution of the interchromophore distance is narrow while the orientational distribution of the two chromophores is quite broad.

(23) Sisido, M.; Shimada, K. *J. Am. Chem. Soc.* **1977**, *99*, 7785.

Scheme I

Table III. Comparison of Excitation Hopping Rates (s^{-1})

	ω,[a]	ω',[b]	$\langle\omega'\rangle$,[c]	$\langle\omega''\rangle$,[d]
N3	1.8×10^8	1.7×10^8	1.8×10^8	4.6×10^8
N5	4.1×10^7	1.0×10^8	5.6×10^8	3.5×10^8
N7	1.9×10^7	3.8×10^7	1.2×10^8	6.9×10^7
N12	6.8×10^6	—	—	—

[a] Experimentally obtained values as in Table II. [b] Rate constants calculated by eq 9a where R_0 = 13 Å and R = 8.41 Å (N3), 9.15 Å (N5), and 10.79 Å (N7). [c] Ensemble-averaged rate constants based on eqs 9a and 13. [d] Ensemble-averaged rate constants based on eqs 9b and 13.

Discussion

The present results clearly indicate that excitation hopping takes place between the two naphthyl moieties attached to both ends of the alkyl chains as detected by the time-resolved measurements of the fluorescence anisotropy (Scheme I). In the incoherent excitation hopping between two identical chromophores, probability that excitation is found at the originally excited site at time t, $P(t)$, can be expressed by eq 8 where ω is the hopping rate

$$P(t) = \tfrac{1}{2}\exp(-2\omega t) + \tfrac{1}{2} \quad (8)$$

constant, which depends on interchromophore distance (R) and mutual orientation of the chromophores.[2d] If we assume the Förster's mechanism for the excitation migration, ω can be written in the form of eq 9a or 9b[2d,12] where τ is the fluorescence lifetime,

$$\omega = 1/\tau(R_0/R)^6 \quad (9a)$$

$$\omega = 1/\tau(R_0'/R)^6\,{}^3/_2\kappa^2 \quad (9b)$$

R_0 is the critical distance commonly used,[24] and κ is the orientation factor defined by eq 10 where θ_{DA} is the angle between the

$$\kappa = \cos\theta_{DA} - 3\cos\theta_D\cos\theta_A \quad (10)$$

transition moment vectors of the donor and the acceptor and θ_D and θ_A are the angles between these transition moments and the direction of R.

If we assume forward and backward excitation hopping between the two identical chromophores, we can derive an equation based on eq 8 (eq 11) where r_0 is a limiting value of r and can be

$$r(t) = \tfrac{1}{2}(r_0 - r_1)\exp(-2\omega t) + \tfrac{1}{2}(r_0 + r_1) \quad (11)$$

estimated from a case where no fluorescence depolarization occurs as in the case of r for EN.[12] The r_0 value for the present system can, thus, be estimated as r_0 = 0.19. The other parameter, r_1, is the anisotropy of fluorescence emitted entirely by the chromophore, which is not originally excited. Comparison of eq 11 with eq 2 yields the relation in eq 12.

$$A = (r_0 - r_1)/2 \qquad B = (r_0 + r_1)/2 \quad (12)$$

The experimentally observed values of ω are compared with theoretically calculated values of the hopping rate constants in Table III. In the table, the rate constants, ω', were calculated by the Förster's equation (eq 9a) in which R_0 = 13 Å for the pair of the 2-naphthyl moieties[10b] and R was taken as the ensemble-averaged interchromophore distance $\langle R\rangle$ calculated by eq 7: $\langle R\rangle$ = 8.41 Å for N3, R = 9.15 Å for N5, and R = 10.79 Å for N7. Another rate constant, $\langle\omega'\rangle$, was calculated by ensemble averaging over the whole conformation. Here, the rate constant for the ith conformation, ω'_i, was calculated on the basis of eq 9a and R = 13 Å, and the ensemble-averaged hopping rate constants were calculated by eq 13. The ensemble-averaged rate constants, $\langle\omega''\rangle$,

$$\langle\omega'\rangle = \sum_i \omega'_i \exp(-E_i/RT)/\sum_i \exp(-E_i/RT) \quad (13)$$

were similarly calculated as $\langle\omega'\rangle$, but in this case κ^2 was taken into account and eq 9b was used in place of eq 9a to calculate the hopping rate constant for the ith conformation. As a first approximation, we assumed that the direction of the transition dipole lies along the long axis of the naphthalene ring; thus, $\theta_{DA} = \theta_L$. The ensemble-averaged hopping rate constants calculated on the above assumption as well as R_0' = 13 Å are listed in the last column in Table III. Table III indicates that agreement between the experimentally determined ω values and the calculated ω' values is good for N3 and N7, while agreement between the ω values and the $\langle\omega'\rangle$ values or the $\langle\omega''\rangle$ values is poor except N3.

Usually, as the Förster's equation predicts, the transfer rate is dependent on κ. However, its dependence on the transfer rate is not so large for the present set of chromophores. (Note that $\langle\omega'\rangle = 1.8 \times 10^8$ and $\langle\omega''\rangle = 4.6 \times 10^8$ for N3, and $\langle\omega'\rangle = 5.6 \times 10^8$ and $\langle\omega''\rangle = 3.5 \times 10^8$ for N5.) Two points may be taken into account.

(1) The electronic transition responsible for the emission of the naphthyl moiety is in principle forbidden, and such transitions often possess different polarizations for different vibronic transitions in the same electronic band, particularly when a strong transition is located close to the electronic band of interest.[25] The latter may correspond to the ^1L_a band in the case of the naphthyl chromophores. Due to overlap of the different vibronic bands, the measured anisotropy is rather low as shown by r_0 = 0.19 for EN. The overlap between the fluorescence and absorption of the 2-naphthyl moieties may, thus, be characterized by rather poorly defined directions of the emission and the absorption transition dipoles.[25] This situation may lead to "intrinsic averaging" over κ^2 even in the absence of rotational diffusion of the chromophores.[25]

(2) A specific feature of α,ω-bis(*2-naphthyl*)alkanes is that the orientational distribution of the two chromophores is broad. In addition to the intrinsic averaging described above, the broad distribution of orientation of the two naphthyl moieties may enable us to treat Nn as randomly oriented systems.

Close inspection of the observed anisotropy decay curves and the fitting curves in Figure 6 indicates that at short times immediately after excitation the observed decay of $r(t)$ is more rapid than the single exponential function expressed by eq 2 in N5 and N7. This is clearly shown by the upward deviation of the residuals in the fitting of the decay curves for N5 and N7. This means that at the initial stage the hopping rate constant should be higher than that obtained by the fitting procedure based on the single exponential function. It is quite reasonable to assume that the inhomogeneity in ω results from distribution of the interchromophore distance and the initial rapid decay of $r(t)$ arises from the closely located pairs of the chromophores. Note that N3 has a narrow distribution of the interchromophore distance, so that the observed decay rate constant, ω, is in reasonable agreement with the calculated values of ω', $\langle\omega'\rangle$, and $\langle\omega''\rangle$. On the other hand, in N5 and N7, the rate constants calculated through ensemble-averaging are much larger than the observed value of ω. These results can be rationalized by the fact that as shown in Figure 8 N5 and N7 have some significant fractions at shorter distances than the most probable distance.

Acknowledgment. We are grateful to Professor I. Yamazaki and Dr. N. Tamai of Molecular Institute at Okazaki, Japan, for the helpful advice on the construction of the picosecond time-correlated single-photon counting system. We also thank Professor M. Sisido of TIT for allowing us to use his program for drawing contour maps and Dr. H. Yamaguchi of TIT for his active collaboration in making our fluorescence decay analysis program.

Registry No. N3, 14564-87-5; N5, 117203-60-8; N7, 117203-61-9; N12, 102745-34-6; EN, 939-27-5.

(24) Berlman, I. B. *Energy Transfer Parameters of Aromatic Compounds*; Academic: New York, 1973.

(25) (a) Haas, E.; Wilchek, M.; Katchalski-Katzir, E.; Steinberg, I. Z. *Proc. Natl. Acad. Sci.* **1975**, *72*, 1807. (b) Haas, E.; Katchalski-Katzir, E.; Steinberg, I. Z. *Biopolymers* **1978**, *17*, 11.